Published in final edited form as:
J Neurophysiol. 2007 November ; 98(5): 2622–2632.

Electrophysiological Diversity of Layer 5 Pyramidal Cells in the Prefrontal Cortex of the Rhesus Monkey: In Vitro Slice Studies

Yu-Ming Chang and **Jennifer I. Luebke**
Department of Anatomy and Neurobiology, Boston University School of Medicine, Boston, Massachusetts

Abstract

Whole cell patch-clamp recordings were employed to characterize the electrophysiological properties of layer 5 pyramidal cells in slices of the prefrontal cortex (Area 46) of the rhesus monkey. Four electrophysiologically distinct cell types were discriminated based on distinctive repetitive action potential (AP) firing patterns and single AP characteristics: regular-spiking slowly adapting type-1 cells (RS1; 62%), regular-spiking slowly adapting type-2 cells (RS2; 18%), regular-spiking fast-adapting cells (FA; 15%), and intrinsically bursting cells (IB; 5%). These cells did not differ with regard to their location in layer 5 nor in their dendritic morphology. In RS1 cells, AP threshold and amplitude did not change significantly during a 2-s spike train, whereas in RS2 and FA cells, AP threshold increased significantly and AP amplitude decreased significantly during the train. In FA cells, complete adaptation of AP firing was observed within 600 ms. IB cells displayed an all-or-none burst of three to six APs, followed by RS1-type firing behavior. RS1 cells could be further subdivided into three subtypes. Low-threshold spiking (LTS) RS1 cells exhibited an initial doublet riding on a depolarizing potential at the onset of a spike train and a prominent depolarizing afterpotential (DAP); intermediate RS1 cells (IM) exhibited a DAP, but no initial doublet, and non-LTS RS1 cells exhibited neither a DAP nor an initial doublet. RS2 and FA cells did not exhibit a DAP or initial doublets. The distinctive firing patterns of these diverse layer 5 pyramidal cells may reflect different roles played by these cells in the mediation of subcortical neuronal activity by the dorsolateral PFC.

INTRODUCTION

The primate dorsolateral prefrontal cortex (PFC) plays an important role in the mediation of higher-order cognitive abilities such as planning and working memory (Fuster 1997; Milner 1995; Petrides 2000a,b). Both layer 2/3 cortico-cortical connections and a closed loop layer 5 cortico-striatal-thalamic-cortical circuit are involved in mediation of these abilities (for review, Alexander et al. 1986; Cavada et al. 2000; Owen 1997). In vivo single- and multiple-unit recording studies in monkeys have established that sustained alterations in action potential (AP) firing rates of prefrontal cortical pyramidal cells play a key role in encoding information during the performance of working memory tasks (Constantinidis et al. 2001; Funahashi et al. 1989; Fuster 1997; Goldman-Rakic 1995), rule learning (Asaad et al. 1998; Pasupathy and Miller 2005), and set shifting (Mansouri et al. 2006). Although little is known about the role of layer 5 pyramidal cells per se in the execution of working memory tasks, it is well established that these cells project densely to the head of the caudate nucleus (Cavada et al. 2000; Eblen and Graybiel 1995; Kemp and Powell 1970), which in turn has been demonstrated to play an important role in the mediation of spatial working memory (Hikosaka et al. 1989; Levy et al. 1997; Postle and D'Esposito 1999).

Address for reprint requests and other correspondence: J. I. Luebke, M949, Boston University School of Medicine, 85 E. Newton St., Boston, MA 02118, (E-mail: jluebke@bu.edu; voicemail: 617-638-5995; fax: 617-638-5954).

A detailed understanding of the basic electrophysiological and intrinsic AP firing properties of pyramidal cells in different laminae of the dorsolateral PFC is essential to an understanding of the means by which integrated networks of cells in this brain area mediate cognitive functions. We have previously described the intrinsic membrane and AP firing properties of layer 2/3 pyramidal cells in PFC slices prepared from both young and aged rhesus monkeys (Chang et al. 2005). In addition, there are several published studies of the intrinsic electrophysiological properties of nonpyramidal cells in slices from monkey PFC (Gonzalez-Burgos et al. 2005a,b; Krimer et al. 2005; Povysheva et al. 2006; Zaitsev et al. 2005). By contrast, nothing is known about the firing patterns and other basic electrophysiological characteristics of layer 5 pyramidal cells in the non-human primate PFC. However, a number of in vivo and in vitro studies of layer 5 pyramidal cells from diverse areas of the rodent and cat neocortex have demonstrated that these cells can be broadly classified as either regular-spiking slowly adapting (RS) or intrinsically bursting (IB) types based on their repetitive AP firing properties (Agmon and Connors 1989; Connors et al. 1982; Schwindt et al. 1997; Silva et al. 1991; Stafstrom et al. 1984; Yang et al. 1996). The firing pattern of RS cells is characterized by relatively long-duration APs followed by a complex of after-hyperpolarizations (AHPs) and by slow spike frequency adaptation in response to sustained depolarizing input, whereas IB cells generate bursts of three or more APs followed either by regular spikes or by repetitive bursts (Chagnac-Amitai et al. 1990; Connors and Gutnick 1990; McCormick et al. 1985). Some studies have further subdivided RS cells into RS1 and RS2 subgroups based primarily on the absence or presence of changes in AP threshold and degree of adaptation across a sustained train of APs (Agmon and Connors 1992; Degenetais et al. 2002). Under this classification scheme, RS1 cells exhibit a constant AP firing threshold and little spike frequency adaptation during a train, whereas RS2 cells exhibit a progressive increase in both threshold and spike frequency adaptation over the course of a train. Two additional categories of cells, regular-spiking fast-adapting cells, which present an initial train of 3–11 spikes followed by a depolarizing plateau, and noninactivating bursting cells, which present all-or-none bursts of 3–8 spikes, which do not inactivate, have also been described in the rat prefrontal cortex (Degenetais et al. 2002) and cat association and sensorimotor cortices (Nishimura et al. 1996; Nunez et al. 1993).

By contrast to the numerous studies demonstrating electro-physiologically distinct populations of layer 5 pyramidal cells in rodents and cats, few studies have directly addressed the issue of whether similar cell populations exist in the primate. However, some insight into this question has been provided by electrophysiological studies in in vitro slices prepared from epileptogenic human neocortical tissue excised as a treatment for intractable epilepsy (Avoli and Olivier 1989; Foehring and Wyler 1990; Foehring et al. 1991; Tasker et al. 1996). For example, Avoli and Olivier (1989) have reported the presence of RS cells in deep layers of the human neocortex. Subsequent studies described the electrophysiological properties of neocortical pyramidal cells across laminae 2–6 as low-threshold spiking (LTS) and RS (also termed non-LTS) (Foehring and Wyler 1990; Foehring et al. 1991; Tasker et al. 1996). LTS cells were described as firing two or three fast APs (supported by Ca^{2+}-dependent low-threshold depolarizing potential) followed by regular spiking behavior, which included marked spike frequency adaptation (Foehring et al. 1991; Tasker et al. 1996).

Given the significant benefits of the monkey over other species in terms of modeling human brain structure and function, the impossibility of studying human brain tissue free from pathology, the role of the cortico-striatal-thalamic-cortical circuit in the mediation of executive functions, and the lack of detailed information on the properties of layer 5 pyramidal cells in the non-human primate, the current study was undertaken to characterize the intrinsic membrane and AP firing characteristics of these cells in the rhesus monkey PFC.

METHODS

Experimental subjects

Eight young (5–12 yr old, 5 female, 3 male) rhesus monkeys (*Macaca mulatta*) were obtained from the Yerkes National Primate Research Center at Emory University and subsequently maintained at the Boston University Laboratory Animal Science Center (LASC) in strict accordance with animal care guidelines as outlined in the National Institutes of Health *Guide for the Care and Use of Laboratory Animals* and the U.S. Public Health Service *Policy on Humane Care and Use of Laboratory Animals*. Both the Boston University LASC and the Yerkes Center are fully accredited by the Association for Assessment and Accreditation of Laboratory Animal Care and all procedures were approved by the Institutional Animal Care and Use Committees (IACUC) of both institutions.

Preparation of slices

Coronal brain slices were obtained from monkeys perfused as part of other on going studies. Monkeys were tranquilized with ketamine (10 mg/ml) and then deeply anesthetized with sodium pentobarbital (to effect 15 mg/kg iv). While under deep anesthesia, monkeys were thoracotomized and craniotomies were performed. Thick blocks (10 mm) of the dorsolateral PFC (area 46) containing both the upper and lower banks of the sulcus principalis were obtained by biopsy. After collection of PFC tissue, the monkeys were killed by exsanguination with a 4% paraformaldehyde solution perfused through the ascending aorta. The PFC block was glued onto the cutting stage of a vibrating microtome with cyanoacrylic glue and bathed in oxygenated (95% O_2-5% CO_2) ice-cold Ringer solution (concentrations in mM: 26 $NaHCO_3$, 124 NaCl, 2 KCl, 3 KH_2PO_4, 10 Glucose, 2.5 $CaCl_2$, and 1.3 $MgCl_2$; pH = 7.4, chemicals obtained from Sigma, St. Louis, MO). Coronal 400-μm-thick slices were cut and placed in 26°C, oxygenated Ringer solution and allowed to equilibrate for ≥1 h prior to use. On average 10 intact slices were obtained from each block of the PFC. The time from the beginning of the perfusion of the monkey to obtaining slices of PFC was ~10–15 min. At the time of recording, a single slice was positioned under a nylon mesh in a submersion type slice-recording chamber and constantly superfused with 26°C, oxygenated Ringer solution at a rate of 2–2.5 ml/min.

Whole cell current-clamp recordings

Layer 5 pyramidal cells in the lower bank of the sulcus principalis (Fig. 1) and located ~1 mm below the pial surface were visually identified with a Nikon E600 infrared-differential interference contrast (IR-DIC) microscope (MicroVideo Instruments, Avon, MA). Standard, tight-seal whole cell patch-clamp recordings (Chang et al. 2005;Luebke and Rosene 2003) were made with electrodes fabricated on a Flaming/Brown horizontal micropipette puller (Model P-87, Sutter Instruments, Novato, CA) from nonheparinized microhematocrit capillary tubes (Fisher, Pittsburgh, PA). Recording pipettes were filled with a potassium aspartate (KAsp) internal solution containing (in mM) 100 KAsp, 15 KCl, 3 $MgCl_2$, 5 EGTA, 10 Na-HEPES, 2 MgATP, 0.3 NaGTP, and 1% biocytin (pH = 7.4, chemicals obtained from Fluka). The electrodes had a final resistance of 3–6 MΩ in the external Ringers solution. Experiments were performed with List EPC-7 and EPC-9 patch-clamp amplifiers and "Pulse" acquisition software from HEKA Electronik (Lambrecht). Recordings were low-pass filtered at 10 kHz, and access resistance was monitored throughout each experiment.

Characterization of passive membrane and AP firing properties

Cells were recorded in the current-clamp mode throughout the course of all experiments. Resting membrane potential was determined by measuring the membrane voltage in the absence of current input. Cells were classified based on their membrane voltage responses to

a series of 2-s current steps (7 steps, ranging from +30 to +330 pA in 50-pA increments) applied from a potential of −70 mV. To determine passive membrane and single AP characteristics, a series of 200-ms hyperpolarizing and depolarizing current steps (11 steps, ranging from −120 to +80 pA in 20-pA increments) were applied to the cell from a potential of −70 mV. Input resistance for each cell was determined by the slope of the best-fit line through a voltage-current (*V-I*) graph. The membrane time constant (tau) was determined by fitting the membrane potential response to a small hyperpolarizing pulse to a single-exponential function. Single AP characteristics, including amplitude, threshold, and kinetics (rise time, duration at half-amplitude, and fall time) were analyzed. The first AP produced by the 200-ms current-clamp series was used for single AP measurements. The threshold for firing was measured by expanding the time scale of the digitized trace in the PulseFit oscilloscope window to 1 ms per gradation and, using a linear measurement software function, measuring the voltage at the point in the trace when upward deflection begins. Maximal AP amplitude was measured from threshold to the peak of the spike on the voltage axis. Duration at 1/2 maximal amplitude was measured at half-amplitude from threshold to peak, whereas rise time and decay time were measured as the duration from threshold to peak amplitude and peak to the beginning of the fast AHP, respectively. AHP amplitudes were measured from baseline (membrane potential during prepulse) to maximal amplitude. Frequency-current (*f-I*) plots were generated by plotting the frequency of APs generated versus depolarizing current step amplitude. To quantitatively compare differences in AP changes of RS1, RS2, and FA cells during repetitive firing, AP amplitudes, thresholds, and interspike intervals (ISIs) over the course of a 280-pA 2-s depolarizing step were also measured. All electrophysiological data were initially analyzed using the “Pulse-Fit” analysis program (HEKA Elektronik; Lambrecht), and further analyzed with “Igor Pro” software (WaveMetrics, Lake Oswego, OR). Only cells that had a resting membrane potential of less than −55 mV, stable access resistance over the course of the recording, and an AP overshoot were included in analyses. Differences in electrophysiological parameters between cell types were analyzed using the Student’s *t*-test (2 tailed) with significance defined at $P < 0.05$. Error bars in all figures represent SE.

Biocytin filling and Alexa-streptavidin labeling of pyramidal cells

Cells from which recordings were obtained were simultaneously filled with biocytin. After recording, slices were transferred to a solution of 4% paraformaldehyde in 0.1M phosphate buffer (PB), pH 7.4, and kept at 4°C overnight. The following day, slices were rinsed in PB (3 × 10 min) and then placed in 0.1% triton x-100/PB at 26°C for 2 h, after which they were incubated overnight at 4°C in Streptavidin-Alexa Fluor 488 conjugate (1:1,000, Vector Labs, Burlingame, CA). Filled cells were serially imaged using a Zeiss LSM 510 confocal laser scanning microscope (Jena, Germany) with a 10× plan-neofluor 0.3 n.a. objective and with a 2× digital zoom. Only cells that met the following selection criteria were further analyzed for quantification of morphological characteristics: the presence of an intact soma, the cell body was located in layer 5, the dendritic tree of the pyramidal cell was filled completely and the main branch of the apical dendrite was not cut, and a reasonable distance between individual filled neurons allowed for unambiguous determination of the exact origin of every filled dendritic segment. After scanning, cells were reconstructed and quantitatively analyzed using Neurolucida software (MicroBrightField, Willistone, VT).

RESULTS

Data were obtained from a total of 74 visually identified layer 5 pyramidal cells in in vitro slices of Area 46 prepared from eight young rhesus monkeys. A representative slice and representative biocytin-filled pyramidal cells from which recordings were obtained are shown in Fig. 1. Three types of regular-spiking (RS) cells and one type of intrinsically bursting cell were discriminated based on different characteristic sustained repetitive AP firing patterns

elicited by 2-s depolarizing current pulses (Fig. 1*B*). Sixty-two percent of the cells were classified as regular-spiking slowly adapting type-1 (RS1) cells which displayed little or no change in AP threshold or amplitude across a depolarizing current step. Eighteen percent of the cells were classified as regular-spiking slowly adapting type-2 (RS2) cells, which displayed progressively and significantly increasing AP threshold and decreasing AP amplitude over the course of a depolarizing current step. Fifteen percent of the cells were classified as regular-spiking fast-adapting (FA) cells, which fired a short train of APs that adapted rapidly over the course of a depolarizing current step. Finally, 5% of the cells (4 of 74) were classified as intrinsic bursting (IB) cells. A summary of the distinctive electrophysiological properties of these 4 cell types is provided in Table 1.

Morphological properties of layer 5 pyramidal cells

A total of 25 layer 5 pyramidal cells were scanned with confocal microscopy (15 RS1, 5 RS2, 4 FA, and 1 IB). Each of these cells had an intact soma (allowing unambiguous determination of the depth of the cell within layer 5), and 15 of the cells met stringent criteria for detailed analysis of dendritic branching structure (6 RS1, 4 RS2, 4 FA, and 1 IB; Table 2). Given that only one of the four IB cells recorded from was intact, it was not possible to determine, in the present study, whether IB cells differ substantially from regular-spiking cells. The one reconstructed IB cell had a superficially located soma, in layer 5A, and had a less extensive dendritic arbor than did the other cell types (Fig. 1*C*, Table 2). There was no apparent relationship between the types of RS cells and depth in layer 5 as the somata of cells of each type were located across the depth of layer 5 (e.g., their somata were located between ~900 and 1,500 μm from the pial surface; Fig. 1*C*). The three different RS cell types did not differ with regard to numbers of basilar and apical dendritic branches nor in the total length of basilar and apical dendrites (Table 2). The single significant difference with regard to morphology was that FA cells exhibited significantly larger cell bodies than did RS1 or RS2 cells ($P < 0.03$).

Repetitive AP firing properties of layer 5 pyramidal cells

RS1 CELLS—The majority of the cells in this study (62%; 46/74) were classified as RS1 type cells, which exhibited a fairly constant AP firing threshold across a given depolarizing current step (Fig. 1*B* and Fig. 2*A*). RS1 cells were further categorized into three subgroups based on the presence or absence of an AP doublet riding on a depolarizing envelope at the onset of a spike train and the presence or absence of a DAP after the first AP spike (Fig. 3). Fifty-nine percent (27/46) of RS1 cells exhibited an initial AP doublet and a prominent DAP and were classified as LTS) (Fig. 3, *A1*, *B1* and *C1*) following the criteria established by Foehring et al. (1991) and Tasker et al. (1996). Previous work has determined that the observed depolarizing envelope in LTS cells (Fig. 3*B1*, *top*) is due to the mixed contribution of a low-threshold T-type calcium current and I_h (Foehring and Wyler 1990;Tasker et al. 1996;Yang et al. 1996). In this study, the presence of an initial doublet and a DAP were associated such that all cells that exhibited doublets also exhibited DAPs (RS1-LTS cells). Neurons that displayed a prominent DAP but no initial doublets (13%; 6/46) were classified as intermediate cells (IM; Fig. 3, *A2*, *B2*, and *C2*) as established in rat layer 5–6 pyramidal cells (Yang et al. 1996). RS1 cells displaying *neither* an initial doublet *nor* a DAP (28%; 13/46) were classified as non-LTS cells following the classification of Tasker et al. (1996) (Fig. 3, *A3*, *B3*, and *C3*). There were no statistical differences in intrinsic membrane properties and repetitive or single AP properties between the subclasses of RS1 cells (data not shown), therefore data from all RS1 subtypes were pooled.

The repetitive AP firing characteristics of each of the three different RS cell types are depicted graphically in Fig. 4. RS1 cells exhibited an average 1.0 ± 0.2 mV increase in AP threshold during a train of spikes (elicited by a 2-s, 280-pA current step) that represents an increase of 2.5 ± 0.6% (range = 0–8.4%). In addition, RS1 cells exhibited little change in AP amplitude

during the train of spikes with an average decrease of 3.5 ± 0.6 mV, representing a 4.6 ± 0.8% change (range = 0.5–12%). Adaptation of firing was assessed by measuring ISIs from 100 ms after the onset of the depolarizing pulse to the last ISI over a 2-s train of spikes (38 ± 4.3% increase in ISI). The frequency of AP firing elicited by a 280-pA depolarizing current step in RS1 cells was 17.5 ± 0.7 Hz. Finally, all RS1 cells exhibited a depolarizing "sag" in response to a hyperpolarizing current pulse of −120 pA (Fig. 2*A*, *top*). This sag, which represents activation of an H current, had a mean amplitude of 3.6 ± 0.5 mV in RS1 cells.

RS2 CELLS—RS2 cells were the second most prevalent cell type observed (18%; 13/74). These cells were characterized by a steadily and significantly increasing AP firing threshold and decreasing AP amplitude across a given depolarizing current step (Fig. 2*B* and Fig. 4). RS2 cells exhibited an average 4.2 ± 0.48 mV increase in AP threshold during a train of spikes elicited by a 2-s, 280-pA current step, which represents an increase of 12.2 ± 1.4% (range = 5.7–21.1%). RS2 cells also exhibited a significant decrease in AP amplitude during the train of spikes, with an average decrease of 13.6 ± 2.2 mV, which is a 19.9 ± −3.6% change (range = 2.5–44.7%). The change in AP threshold across a 2-s train was significantly greater in RS2 compared with RS1 type cells ($P < 0.001$), and the change in amplitude was also significantly greater ($P < 0.001$). RS2 cells were similar to RS1 cells with regard to adaptation of spike firing over a 2-s train (42.2 ± 8.4% increase in ISI). The frequency of AP firing elicited by a 280-pA depolarizing current step in RS2 cells was not significantly different from the RS1 type with a mean frequency of 17.5 ± 1.6 Hz. By contrast to the majority of RS1 cells, none of the RS2 cells exhibited a DAP or an initial doublet in response to a depolarizing current step. However, as with RS1 cells, RS2 cells exhibited a depolarizing sag which had a mean amplitude of 2.8 ± 0.6 mV (Fig. 2*B*, *top*; not significantly different from RS1).

FA CELLS—Eleven cells (15%) were classified as FA cells (Fig. 2*C* and Fig. 4). The firing patterns elicited by increasing depolarization of FA cells tended to be more variable than the sustained AP discharge of RS1 and RS2 cells. In general, however, FA cells fired a brief train of 2–10 APs followed by a small depolarizing plateau in response to depolarizing current pulses of 30–280 pA (Fig. 2*C*, gray arrows). FA cells were similar to RS2 cells (and differed from RS1 cells) in that they were characterized by a steadily increasing AP firing threshold. Thus FA cells exhibited a 5.2 ± 1.7 mV increase in AP threshold (a 13.7 ± 3.9% increase, range 3.6–31.5%) over the course of a train elicited by a 280-pA current step. Further, FA cells resembled RS2 cells in that they exhibited a significant 8.1 ± 2.7 mV decrease in AP amplitude (a 12.3 ± −4.1% decrease, range 4.1–23.2%) across a train of spikes elicited by the 280-pA step. The change in amplitude across the step was significantly greater in FA compared with RS1 ($P < 0.05$) but not RS2 type cells ($P < 0.1$). Most strikingly, FA cells exhibited prominent adaptation of firing, with complete firing cessation within 600 ms of the onset of the 280-pA depolarizing step in 7 of the 11 FA cells sampled. In the other three FA cells, sporadic AP firing was observed after the initial train of spikes (e.g., Fig. 2*C*). As with the other two cell types, FA cells exhibited adaptation of firing during a train with the change in ISI over 600 ms being a 56.8 ± 5.9% increase (range: 42–80%). FA cells showed a greater change in ISI over the duration of an evoked train (~600 ms) than did either RS1 or RS2 cells ($P < 0.04$). However, the frequency of firing by FA cells during a train of spikes elicited by the 280-pA step was 16 ± 1.9 Hz and not significantly different from RS1 and RS2 cells (Fig. 4*D*). Unlike RS1 cells, and similar to RS2 cells, none of the FA cells exhibited a DAP or an initial doublet in response to a depolarizing current step. As with RS1 and RS2 cells, FA cells exhibited a depolarizing sag that had a mean amplitude of 2.8 ± 0.3 mV (Fig. 2*C*, *top*; not significantly different from RS1 or RS2).

IB CELLS—Four cells (5%) were classified as IB cells. These neurons exhibited an all-or-none initial burst of three to six spikes, riding on top of a slow depolarizing envelope, in

response to depolarizing current pulses (Fig. 2*D*). Given the very low number of IB cells in the sample, this cell type was not included in quantitative statistical analyses of repetitive firing properties. At higher current steps, the bursts became less pronounced and were followed by a regular train of AP spikes that did not change significantly in amplitude or threshold across the train. IB cell single APs were followed by a prominent DAP similar to those seen in RS1 cells. As with the other cell types, IB cells exhibited a depolarizing sag in response to hyperpolarizing current steps (Fig. 2*D*, *top*).

AHP properties of layer 5 pyramidal cells

In each of the four cell types, single APs were followed by both fast (f) and medium (m) AHPs; however, in most cases, the mAHP overlapped with and thus masked the fAHP, resulting in an AHP that appeared to be monophasic or with only a small notch indicative of the fAHP. Thus fAHP amplitudes were not assessed in the present study. RS1 cells exhibited significantly lower mean mAHP amplitude (10.4 ± 0.7 mV) compared with RS2 (14.3 ± 1 mV; $P < 0.004$) cells and a trend toward a lower mean mAHP amplitude than FA cells (12.5 ± 0.9 mV; $P < 0.08$; Fig. 5). The mean mAHP amplitudes of RS2 and FA cells were not significantly different. Each of the cell types exhibited a slow (s) AHP at the offset of a 2-s, 330-pA current pulse. The mean amplitude of the sAHP in RS1 cells was 3.8 ± 0.5 mV, which was significantly greater than that of RS2 cells (1.1 ± 0.4 mV at 280 pA, $P < 0.001$), and FA cells (1.4 ± 0.75, $P < 0.001$; Fig. 5). The sAHP amplitudes of RS2 and FA cells were not significantly different.

Single AP properties of layer 5 pyramidal cells

Single AP properties were evaluated from APs evoked by a 200-ms suprathreshold depolarizing current pulse. Although the mean AP threshold was not significantly different between RS1 (−42.5 ± 0.6 mV) and FA cell types (−43.9 ± 1.3 mV), it was significantly more depolarized in the RS2 cells (−40.6 ± 0.6 mV) compared with both RS1 and FA cells ($P < 0.04$; Fig. 6). Single AP amplitude was not different between RS2 (79.7 ± 2.2 mV) and FA cells (80.1 ± 2.2 mV); however, their amplitude was significantly greater in RS1 cells (85.8 ± 1.2) compared with both RS2 and FA cells ($P < 0.04$). There were no significant differences in AP kinetics among any of the three cell types (data not shown). The duration of APs at half-maximum amplitude was 1.4 ± 0.06 ms (RS1), 1.5 ± 0.09 ms (RS2), and 1.5 ± 0.1 ms (FA). The mean AP rise times were 0.79 ± 0.02 ms (RS1), 0.87 ± 0.05 ms (RS2), and 0.88 ± 0.05 ms (FA), and the mean AP fall times were 2.3 ± 0.1 ms (RS1), 2.6 ± 0.2 ms (RS2), and 2.8 ± 0.2 ms (FA).

Passive membrane properties of layer 5 pyramidal cells

As shown in Fig. 7, RS1 cells exhibited significantly lower input resistances than RS2 cells ($P < 0.03$) with mean values of 143 ± 7 MΩ (RS1) and 179 ± 13 MΩ (RS2). FA cells did not differ significantly from either RS1 or RS2 cells with a mean input resistance of 161± 13.4 MΩ. Resting membrane potential did not differ among the three cell types with RS1 cells having a mean resting membrane potential of −65.5 ± 1 mV compared with −65.7 ± 1.9 mV for RS2 cells and −65.9 ± 1.5 mV for FA cells. Membrane time constants also did not significantly differ among cell types with mean values of 22.9 ± 1.9 ms (RS1), 26.3 ± 2.6 ms (RS2), and 22.4 ± 2.2 ms (FA).

DISCUSSION

The present study was undertaken to identify and characterize electrophysiologically distinct classes of layer 5 pyramidal cells in the rhesus monkey PFC for the first time. Three classes of regular spiking cells were discriminated based primarily on distinctive repetitive AP firing patterns and spike characteristics: RS1, RS2, and, for the first time in an in vitro study, FA cells. In addition, one type of intrinsically bursting neuron was observed, albeit very rarely.

Overall, the data support the idea that the electrophysiological properties of layer 5 pyramidal cells are largely conserved across species and cortical areas, although minor differences in the specific electrophysiological properties and relative proportion of the different classes (RS1, RS2, FA, IB) do exist, as detailed in the following text.

Morphological properties

Interestingly, the three types of regular spiking cells did not differ with regard to their location within the depth of layer 5 nor with regard to their dendritic morphology. It was not possible in the present study to characterize the morphological properties of IB cells due to their scarcity, although it is interesting to note that the one reconstructed IB cell had a cell body located superficially, in layer 5A, and had a less extensive dendritic arbor than did the other cell types. Further studies are required to determine whether IB cells are morphologically distinct from regular-spiking cell types in the primate prefrontal cortex. Previous studies have shown a relationship between morphological properties and specific AP firing patterns in layer 5 neurons in rat visual (Kasper et al. 1994; Larkman and Mason 1990; Mason and Larkman 1990) and prefrontal cortex (Yang et al. 1996) and in ferret prefrontal cortex (Wang et al. 2006). For example, Kasper et al. (1994) showed that in the rat visual cortex bursting neurons have thick tufted apical dendrites, whereas RS neurons have slender apical dendrites without a terminal tuft. More recently, Wang and colleagues demonstrated a subpopulation of layer 5 prefrontal cortical neurons in the ferret that possess dual apical dendrites and exhibit nonaccomodating firing properties. We did not observe neurons with such dual dendrites in the present study; further studies are required to determine whether this type of layer 5 pyramidal cell is present in the monkey prefrontal cortex.

Repetitive AP firing properties

RS1—The repetitive AP firing properties of RS1 cells in the monkey are similar to those previously reported in the mouse (Agmon and Connors 1992) and rat (Degenetais et al. 2002). Thus as in the mouse, monkey RS1 cells exhibit unchanging AP thresholds and amplitudes during sustained firing evoked by a given current step, exhibit modest adaptation of firing during a train and often fire an initial doublet at the onset of a train. In the rat, RS1 cells have been shown to exhibit each of these characteristics and, in addition, to exhibit a DAP after the initial AP spike of a doublet. This DAP has been reported to be present in pyramidal cells from a number of neocortical areas in a variety of animal (Kang and Kayano 1994; Mason and Larkman 1990; Montoro et al. 1988) and human (Foehring et al. 1991; Tasker et al. 1996) brain areas. It has been suggested that the lack of significant firing rate adaptation in RS1 cells may be associated with the presence of this DAP and a depolarizing “sag” potential, both of which, in previous rodent studies, have been reported to exist only in RS1 type cells (Degenetais et al. 2002; Kang and Kayano 1994). Our results are not consistent with this idea because although (as in the rodent) the majority of monkey RS1 but no RS2 cells exhibited a DAP, there was no significant difference in the amount of firing adaptation between RS1 subgroups or between RS1 and RS2 cells. In addition, there was no significant difference in the amplitude of the depolarizing sag in the different RS1 cell subtypes.

Despite the similarity of findings in this primate and previous rodent and cat studies, subtle differences between the RS1 cell population in these species do exist. For example, Degenetais et al. (2002) report that, in the rat in vivo, all RS1 cells exhibit a DAP and an initial doublet at the beginning of a train of spikes. In the monkey population of RS1 cells sampled here, most but not all exhibited a DAP and only RS1 LTS cells fired an initial doublet. All cells that fired an initial doublet showed clear signs of a DAP; however, six cells with DAPs did not exhibit an initial doublet. It is likely that the cells in the present study with DAPs, but no doublets correspond to cells described as intermediate (IM) cells in layer 5 of the rat PFC (Yang et al. 1996). These IM cells exhibit characteristics of RS1 cells, such as steady AP threshold, steady

ISIs, and the presence of a DAP, but lacked an initial doublet. The RS1 non-LTS cells seen in the monkey PFC fit the general criterion for RS1 cells established in rodents and cats in that they display a constant AP threshold across a given current step but differ from earlier descriptions in that they lack an initial doublet and DAP. However, these cells are not otherwise electrophysiologically different from RS1 cells that do exhibit initial doublets and DAPs.

RS2—The repetitive AP firing patterns of RS2 cells in the monkey PFC are generally similar to those previously reported in the rat. Thus there is a significant increase in AP threshold across time in response to a depolarizing current stimulus (Degenetais et al. 2002) and an absence of a DAP (Degenetais et al. 2002; Yang et al. 1996). However, as with RS1 cells, there are subtle differences between characteristics of RS2 cells in rodents and monkeys. For example, although not specifically reported in other species, monkey RS2 cells exhibit a dramatic decrease in AP spike amplitude across time during sustained discharge. In addition, although none of the monkey RS2 cells exhibited an initial doublet, rat RS2 cells have been reported to occasionally exhibit an initial doublet or triplet in response to a depolarizing current stimulus (Degenetais et al. 2002; Tseng and Prince 1993; Van Brederode and Snyder 1992). Degenetais et al. (2002) report that RS2 but not RS1 type cells exhibit significant spike frequency adaptation over the course of a depolarizing current pulse. In monkey RS2 cells, however, although increasing thresholds were observed, no significant increase in spike frequency adaptation (as measured by ISI durations across a given train) was seen. Hence, in the present study RS1 and RS2 cells did not differ with regard to degree of adaptation of firing during a train.

It is interesting to note that in the mouse, Agmon and Connors (1992) observed that whereas RS1 cells were found throughout the layers of the neocortex, RS2 type cells were found only in layer 5. This differs from observations in the monkey, where RS2 cells are the predominant cell type in layer 2/3 (unpublished observations) and in the rat where RS2 type cells are also found in layer 2/3 (Degenetais et al. 2002). Indeed, the RS1 cell type was the predominant cell type observed in layer 5 in the present study.

FA—Previously, fast-adapting RS cells, which are characterized by an initial short train of spikes followed either by a complete cessation of/or sparsely intermittent AP firing in response to a depolarizing current pulse, have only been seen in in vivo recordings such as in the cat association and rat prefrontal cortex (Degenetais et al. 2002; Nunez et al. 1993). This study describes the FA cell in an in vitro slice preparation for the first time. As previously described in the cat and rat, a small slow depolarizing membrane plateau is present after the initial train of spikes. In general, FA cells were more similar to RS2 than to RS1 cells in that they displayed significantly increased AP thresholds and decreased AP amplitudes across a train and did not exhibit a DAP or an initial doublet. In addition, the mAHP and sAHP amplitudes of FA and RS2 cells did not differ significantly (although both RS2 and FA differed from RS1 cells). Thus FA and RS2 cells differed only with regard to degree of adaptation. It is possible that FA cells represent a further subtype of RS2 cell or perhaps simply represent a different firing modality of RS2 cells.

AHP properties

One important mechanism by which AP firing rates can be modulated is through alterations in the characteristics of medium and slow AHPs (reviewed in Sah 1996;Sah and Davies 2000). Furthermore, increases in sAHP amplitude are associated with decreased firing rates in hippocampal pyramidal cells (reviewed in Thibault et al. 1998). Monkey RS1 cells demonstrated a significantly lower mAHP amplitude than RS2 and FA cells, yet RS1 cells did not exhibit shorter ISI durations or faster AP firing rates compared with RS2 or FA cells. One possible explanation for this apparent discrepancy may be that in RS1 cells, the higher

amplitude sAHP (relative to those seen in RS2 and FA cells) may act to counteract differences in AP firing frequency that might otherwise result from decreased mAHP amplitude. Further voltage-clamp studies of AHPs in these cells are required to resolve these issues.

Single AP properties

Single AP threshold was significantly lower in RS1 compared with RS2 cells and single AP amplitude significantly greater in RS1 than both RS2 and FA cells. These results are consistent with those observed in the rat. Tseng and Prince (1993) report that in RS1-like cells (classified in their study as "RS") APs exhibited increased amplitudes, as measured from threshold to peak, compared with RS2-like cells (classified in their study as "adapting"). Although Degenetais et al. (2002) did not report significant differences between RS1 and RS2 cells combined as a group versus FA cells, there appeared to be a trend showing that FA cells had lower spike amplitudes. Such differences may reflect a difference in the characteristics of voltage-activated sodium channels in specific cell types. Further voltage-clamp data studies are required to examine this issue.

Few IB cells were observed

The existence of intrinsically bursting cells in layer 5 neocortical pyramidal cells has been demonstrated in numerous rodent (e.g., Agmon and Connors 1992; Connors et al. 1982; Degenetais et al. 2002; Tseng and Prince 1993; Yang et al. 1996) and cat (Baranyi et al. 1993; Nishimura et al. 1996; Nunez et al. 1993) studies. Intrinsically bursting cells have been variously categorized as IB (Connors and Gutnick 1990; Degenetais et al. 2002), repetitive oscillatory-bursting (ROB) (Yang et al. 1996), RS_{DAP} (Tseng and Prince 1993), and noninactivating bursting cells (Baranyi et al. 1993). Degenetais and co-workers (2002) have previously grouped ROB, RS_{DAP}, and noninactivating bursting cells as IB cells, and this paper follows this convention.

Only four cells fitting the characteristics of IB cells were observed in the present study. One possible explanation for the paucity of observed IB cells is that the IB firing pattern seems to be state dependent. Previous studies have demonstrated that the number of reported IB cells in in vivo rodent experiments is inversely correlated with the state of anesthesia (reviewed in Contreras 2004). Nevertheless, rodent studies using in vitro slice preparations similar to that used in the current study report an average of 12–30% of recorded cells as IB (Connors et al. 1982; Tseng and Prince 1993; Yang et al. 1996). A second possible, although unlikely, explanation for this observation is that although recordings were made through the depth of layer 5, many of the cells were located within the more superficial strata layer 5A. Previous studies indicate that IB cells and noninactivating bursting cells are predominantly found in layer 5B and layer 6 (e.g., Degenetais et al. 2002; Mason and Larkman 1990; Nowak et al. 2003). However, it should be noted that a recent study in the rat somatosensory cortex reported that ~29% of pyramidal cells in layer 5A exhibited intrinsically bursting activity (Schubert et al. 2005).

Most plausibly, it is likely that IB cells are rare in the primate neocortex in contrast to rodents or cats; indeed, Avoli and Olivier (1989), Foehring and coworkers (1991), and Tasker and coworkers (1996) all reported a similar absence of IB cells in layers 2–6 of the human neocortex. As discussed in the preceding text, RS1-LTS cells in the current study fired an initial doublet supported by a depolarizing envelope, likely caused by a low-threshold calcium current and I_h, followed by a regular spike firing pattern. Although the majority of previous studies have categorized such firing patterns as regular spiking, at least one study has classified LTS cells as IB cells (Yang et al. 1996). Under such criteria, 37% layer 5 PFC pyramidal cells (27/74) in the monkey could be considered "bursting" cells (Yang et al. 1996).

Conclusions

This study has established the presence of four distinct electrophysiological classes of layer 5 pyramidal cells in the rhesus monkey PFC. The cell classes can be differentiated primarily based on their characteristic repetitive AP firing responses to depolarizing current steps. Thus FA cells show very rapid adaptation of firing across 2 s, whereas RS1 and RS2 cells do not. RS1 and RS2 cells can be differentiated primarily on the basis of differential changes in AP threshold and amplitude over the course of an evoked train with RS2 but not RS1 cells demonstrating significant changes in these parameters. IB cells were classified based on the large “burst” of four to six APs riding on a large depolarizing plateau. In addition, most RS1 and all IB cells differ from both RS2 and FA cells in that they exhibit a prominent DAP.

The observed differences in firing patterns and other electrophysiological properties in these four distinct cell types likely reflect differences in ion channel complement, excitatory and inhibitory synaptic inputs and/or possibly location of their postsynaptic targets. There is evidence that the majority of non-LTS and LTS RS1 cells in layer 5 display very specific anatomical targets and synaptic connections in the rat (Morishima and Kawaguchi 2006). The large majority of layer 5 pyramidal cells projecting to the ipsilateral striatum and pontine structures (CPn) display LTS firing patterns, whereas cells projecting to only the contra- and ipsilateral striatum (CCS) display non-LTS RS1 firing patterns. Whether these distinct classes of cells play different roles in the mediation of executive function by the PFC is unknown. It is important to bear in mind that the electrophysiological properties of layer 5 pyramidal cells may, in vivo, differ substantially from those seen in vitro largely because they are subject to significant modulation, in vivo, by synaptic inputs (that are much reduced in vitro). However, although this caveat is a given, these data do provide important insight into the electrophysiological diversity of layer 5 pyramidal cell classes in the primate prefrontal cortex. Data such as these are arguably necessary (but not sufficient) for predictions regarding the in vivo behavior of individual neurons within complex neocortical circuits.

Given the significant differences in the AP firing patterns of layer 5 pyramidal cells, it could plausibly be predicted that they exhibit different input-output transformation properties during the execution of working memory tasks. If this was true, it may be hypothesized that the fidelity of transmission of inputs would be greatest in RS1 cells (which demonstrate constant AP characteristics during sustained firing), potentially slightly less in RS2 cells (which demonstrate increased threshold and decreased amplitude of APs during sustained firing) and significantly less in FA cells (which adapt very rapidly).

ACKNOWLEDGMENTS

The authors thank Dr. Douglas Rosene for performing perfusions of the monkeys and providing brain tissue from which recordings were obtained. The skillful assistance of Dr. Anne Rocher and Dr. James Nilson and M. Todd-Brown in the reconstruction and analysis of biocytin-filled cells is gratefully acknowledged.

GRANTS This work was supported by National Institute on Aging Grants PO1-AG-00001 and R01-AG-025062.

REFERENCES

Agmon A, Connors BW. Repetitive burst-firing neurons in the deep layers of mouse somatosensory cortex. Neurosci Lett 1989;99:137–141. [PubMed: 2748005]

Agmon A, Connors BW. Correlation between intrinsic firing patterns and thalamocortical synaptic responses of neurons in mouse barrel cortex. J Neurosci 1992;12:319–329. [PubMed: 1729440]

Alexander GE, DeLong MR, Strick PL. Parallel organization of functionally segregated circuits linking basal ganglia and cortex. Annu Rev Neurosci 1986;9:357–381. [PubMed: 3085570]

Asaad WF, Rainer G, Miller EK. Neural activity in the primate prefrontal cortex during associative learning. Neuron 1998;21:1399–1407. [PubMed: 9883732]

Avoli M, Olivier A. Electrophysiological properties and synaptic responses in the deep layers of the human epileptogenic neocortex in vitro. J Neurophysiol 1989;61:589–606. [PubMed: 2709102]

Baranyi A, Szente MB, Woody CD. Electrophysiological characterization of different types of neurons recorded in vivo in the motor cortex of the cat. I. Patterns of firing activity and synaptic responses. J Neurophysiol 1993;69:1850–1864. [PubMed: 8350126]

Cavada C, Company T, Tejedor J, Cruz-Rizzolo RJ, Reinoso-Suarez F. The anatomical connections of the Macaque monkey orbitofrontal cortex. A review. Cereb Cortex 2000;10:220–242. [PubMed: 10731218]

Chagnac-Amitai Y, Luhmann HJ, Prince DA. Burst generating and regular spiking layer 5 pyramidal neurons of rat neocortex have different morphological features. J Comp Neurol 1990;296:598–613. [PubMed: 2358553]

Chang YM, Rosene DL, Killiany RJ, Mangiamele LA, Luebke JI. Increased action potential firing rates of layer 2/3 pyramidal cells in the prefrontal cortex are significantly related to cognitive performance in aged monkeys. Cereb Cortex 2005;15:409–418. [PubMed: 15749985]

Connors BW, Gutnick MJ. Intrinsic firing patterns of diverse neocortical neurons. Trends Neurosci 1990;13:99–104. [PubMed: 1691879]

Connors BW, Gutnick MJ, Prince DA. Electrophysiological properties of neocortical neurons in vitro. J Neurophysiol 1982;48:1302–1320. [PubMed: 6296328]

Constantinidis C, Franowicz MN, Goldman-Rakic PS. Coding specificity in cortical microcircuits: a multiple-electrode analysis of primate prefrontal cortex. J Neurosci 2001;21:3646–3655. [PubMed: 11331394]

Contreras D. Electrophysiological classes of neocortical neurons. Neural Netw 2004;17:633–646. [PubMed: 15288889]

Degenetais E, Thierry AM, Glowinski J, Gioanni Y. Electrophysiological properties of pyramidal neurons in the rat prefrontal cortex: an in vivo intracellular recording study. Cereb Cortex 2002;12:1–16. [PubMed: 11734528]

Eblen F, Graybiel AM. Highly restricted origin of prefrontal cortical inputs to striosomes in the macaque monkey. J Neurosci 1995;15:5999–6013. [PubMed: 7666184]

Foehring RC, Lorenzon NM, Herron P, Wilson CJ. Correlation of physiologically and morphologically identified neuronal types in human association cortex in vitro. J Neurophysiol 1991;66:1825–1837. [PubMed: 1812219]

Foehring RC, Wyler AR. Two patterns of firing in human neocortical neurons. Neurosci Lett 1990;110:279–285. [PubMed: 2325900]

Funahashi S, Bruce CJ, Goldman-Rakic PS. Mnemonic coding of visual space in the primate dorsolateral prefrontal cortex. J Neurophysiol 1989;63:331–349. [PubMed: 2918358]

Fuster, JM. The Prefrontal Cortex: Anatomy, Physiology and Neurophysiology of the Frontal Lobe. 3rd ed.. Philadelphia: Lippencott-Raven; 1997.

Goldman-Rakic PS. Cellular basis of working memory. Neuron 1995;14:477–485. [PubMed: 7695894]

Gonzalez-Burgos G, Krimer LS, Povysheva NV, Barrionuevo G, Lewis DA. Functional properties of fast spiking interneurons and their synaptic connections with pyramidal cells in primate dorsolateral prefrontal cortex. J Neurophysiol 2005a;93:942–953. [PubMed: 15385591]

Gonzalez-Burgos G, Kroener S, Seamans JK, Lewis DA, Barrionuevo G. Dopaminergic modulation of short-term synaptic plasticity in fast-spiking interneurons of primate dorsolateral prefrontal cortex. J Neurophysiol 2005b;94:4168–4177. [PubMed: 16148267]

Hikosaka O, Sakamoto M, Usui S. Functional properties of monkey caudate neurons. III. Activities related to expectation of target and reward. J Neurophysiol 1989;61:814–832. [PubMed: 2723722]

Kang Y, Kayano F. Electrophysiological and morphological characteristics of layer VI pyramidal cells in the cat motor cortex. J Neurophysiol 1994;72:578–591. [PubMed: 7983520]

Kasper EM, Larkman AU, Lubke J, Blakemore C. Pyramidal neurons in layer 5 of the rat visual cortex. I. Correlation among cell morphology, intrinsic electrophysiological properties, and axon targets. J Comp Neurol 1994;339:459–474. [PubMed: 8144741]

Kemp JM, Powell TPS. The cortico-striate projections in the monkey. Brain 1970;93:525–546. [PubMed: 4990231]

Krimer LS, Zaitsev AV, Czanner G, Kroner S, Gonzalez-Burgos G, Povysheva NV, Iyengar S, Barrionuevo G, Lewis DA. Cluster analysis-based physiological classification and morphological properties of inhibitory neurons in layers 2–3 of monkey dorsolateral prefrontal cortex. J Neurophysiol 2005;94:3009–3022. [PubMed: 15987765]

Larkman A, Mason A. Correlations between morphology and electrophysiology of pyramidal neurons in slices of rat visual cortex. I. Establishment of cell classes. J Neurosci 1990;10:1407–1414. [PubMed: 2332787]

Levy R, Friedman H, Davachi L, Goldman-Rakic P. Differential activation of the caudate nucleus in primates performing spatial and nonspatial working memory tasks. J Neurosci 1997;17:3870–3882. [PubMed: 9133405]

Luebke JI, Rosene DL. Aging alters dendritic morphology, input resistance, and inhibitory signaling in dentate granule cells of the rhesus monkey. J Comp Neurol 2003;460:573–584. [PubMed: 12717715]

Mansouri FA, Matsumoto K, Tanaka K. Prefrontal cell activities related to monkeys' success and failure in adapting to rule changes in a Wisconsin Card Sorting Test analog. J Neurosci 2006;26:2745–2756. [PubMed: 16525054]

Mason A, Larkman A. Correlations between morphology and electrophysiology of pyramidal neurons in slices of rat visual cortex. II. Electrophysiology. J Neurosci 1990;10:1415–1428. [PubMed: 2332788]

McCormick DA, Connors BW, Lighthall JW, Prince DA. Comparative electrophysiology of pyramidal and sparsely spiny stellate neurons of the neocortex. J Neurophysiol 1985;54:782–806. [PubMed: 2999347]

Milner B. Aspects of human frontal lobe function. Adv Neurol 1995;66:67–81. [PubMed: 7771312]

Montoro RJ, Lopez-Barneo J, Jassik-Gerschenfeld D. Differential burst firing modes in neurons of the mammalian visual cortex in vitro. Brain Res 1988;460:168–172. [PubMed: 3219569]

Morishima M, Kawaguchi Y. Recurrent connection patterns of corticostriatal pyramidal cells in frontal cortex. J Neurosci 2006;26:4394–4405. [PubMed: 16624959]

Nishimura Y, Kitagawa H, Saitoh K, Asahi M, Itoh K, Yoshioka K, Asahara T, Tanaka T, Yamamoto T. The burst firing in the layer III and V pyramidal neurons of the cat sensorimotor cortex in vitro. Brain Res 1996;727:212–216. [PubMed: 8842400]

Nowak LG, Azouz R, Sanchez-Vives MV, Gray CM, McCormick DA. Electrophysiological classes of cat primary visual cortical neurons in vivo as revealed by quantitative analysis. J Neurophysiol 2003;89:1541–1566. [PubMed: 12626627]

Nunez A, Amzica F, Steriade M. Electrophysiology of cat association cortical cells in vivo: intrinsic properties and synaptic responses. J Neurophysiol 1993;70:418–430. [PubMed: 8395586]

Owen AM. Cognitive planning in humans: neuropsychological, neuroanatomical, and neuropharmacological perspectives. Prog Neurobiol 1997;53:431–450. [PubMed: 9421831]

Pasupathy A, Miller EK. Different time courses of learning-related activity in the prefrontal cortex and striatum. Nature 2005;433:873–876. [PubMed: 15729344]

Petrides M. The role of the mid-dorsolateral prefrontal cortex in working memory. Exp Brain Res 2000a; 133:44–54. [PubMed: 10933209]

Petrides M. Dissociable roles of mid-dorsolateral prefrontal and anterior inferotemporal cortex in visual working memory. J Neurosci 2000b;20:7496–7503. [PubMed: 11007909]

Postle BR, D'Esposito M. Dissociation of human caudate nucleus activity in spatial and nonspatial working memory: an event-related fMRI study. Cogn Brain Res 1999;8:107–115.

Povysheva NV, Gonzalez-Burgos G, Zaitsev AV, Kroner S, Barrionuevo G, Lewis DA, Krimer LS. Properties of excitatory synaptic responses in fast-spiking interneurons and pyramidal cells from monkey and rat prefrontal cortex. Cereb Cortex 2006;16:541–552. [PubMed: 16033926]

Sah P. Ca(2+)-activated K^+ currents in neurons: types, physiological roles and modulation. Trends Neurosci 1996;19:150–154. [PubMed: 8658599]

Sah P, Davies P. Calcium-activated potassium currents in mammalian neurons. Clin Exp Pharmacol Physiol 2000;27:657–663. [PubMed: 10972528]

Schwindt P, O'Brien JA, Crill W. Quantitative analysis of firing properties of pyramidal neurons from layer 5 of rat sensorimotor cortex. J Neurophysiol 1997;77:2484–2498. [PubMed: 9163371]

Schubert D, Kotter R, Luhmann HJ, Staiger JF. Morphology, electrophysiology and functional input connectivity of pyramidal neurons characterizes a genuine layer Va in the primary somatosensory cortex. Cereb Cortex 2006;16:223–236. [PubMed: 15872153]

Silva LR, Amitai Y, Connors BW. Intrinsic oscillations of neocortex generated by layer 5 pyramidal neurons. Science 1991;251:432–435. [PubMed: 1824881]

Stafstrom CE, Schwindt PC, Crill WE. Repetitive firing in layer V neurons from cat neocortex in vitro. J Neurophysiol 1984;52:264–277. [PubMed: 6481432]

Tasker JG, Hoffman NW, Kim YI, Fisher RS, Peacock WJ, Dudek FE. Electrical properties of neocortical neurons in slices from children with intractable epilepsy. J Neurophysiol 1996;75:931–939. [PubMed: 8714665]

Thibault O, Porter NM, Chen KC, Blalock EM, Kaminker PG, Clodfelter GV, Brewer LD, Landfield PW. Calcium dysregulation in neuronal aging and Alzheimer's disease: history and new directions. Cell Calcium 1998;24:417–433. [PubMed: 10091010]

Tseng GF, Prince DA. Heterogeneity of rat corticospinal neurons. J Comp Neurol 1993;335:92–108. [PubMed: 8408775]

Van Brederode JFM, Snyder GL. A comparison of the electrophysiological properties of morphologically identified cells in layers 5b and 6 of the rat neocortex. Neuroscence 1992;50:315–337.

Wang Y, Markram H, Goodman PH, Berger TK, Ma J, Goldman-Rakic PS. Heterogeneity in the pyramidal network of the medial prefrontal cortex. Nat Neurosci 2006;9:534–542. [PubMed: 16547512]

Yang CR, Seamans JK, Gorelova N. Electrophysiological and morphological properties of layers V–VI principal pyramidal cells in rat prefrontal cortex in vitro. J Neurosci 1996;16:1904–1921. [PubMed: 8774458]

Zaitsev AV, Gonzalez-Burgos G, Povysheva NV, Kroner S, Lewis DA, Krimer LS. Localization of calcium-binding proteins in physiologically and morphologically characterized interneurons of monkey dorsolateral prefrontal cortex. Cereb Cortex 2005;15:1178–1186. [PubMed: 15590911]

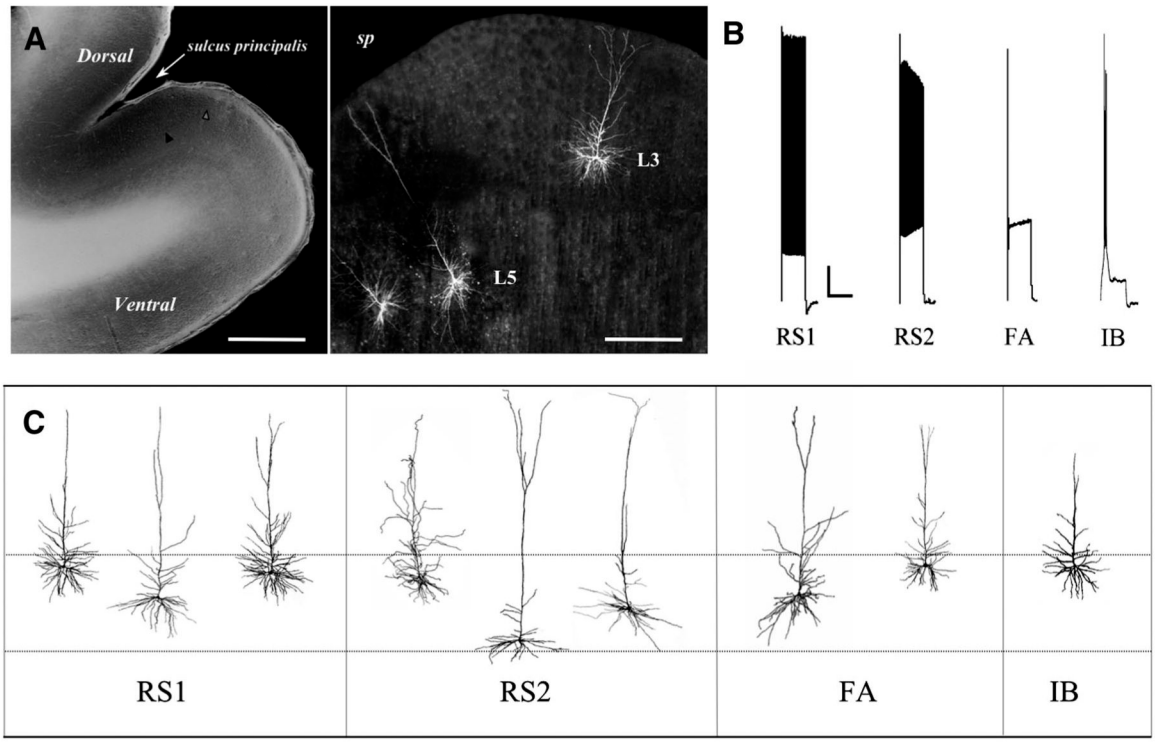

FIG. 1.

A, left: photomicrograph of a typical prefrontal cortex (PFC) slice, Scale bar: 1.2 mm; right panel: higher-magnification view of a PFC with 3 representative biocytin-filled pyramidal cells (2 in layer 5, 1 in layer 2/3). Scale bar: 300 μm. *B*: distinctive action potential (AP) firing patterns elicited by a 2-s, 280-pA depolarizing current step in the 4 types of layer 5 pyramidal cells. Note the progressive decrease in AP amplitude and increase in AP threshold in regular-spiking slowly adapting type-2 (RS2) and regular-spiking fast-adapting (FA) but not regular-spiking slowly adapting type-1 (RS1) cells, and the rapid rate of adaptation in FA cells only. *C*: diagram of representative reconstructed layer 5 pyramidal cells of each electrophysiological class. - - -, approximate boundaries of layer 5 (~900–1,500 μm deep to the pial surface).

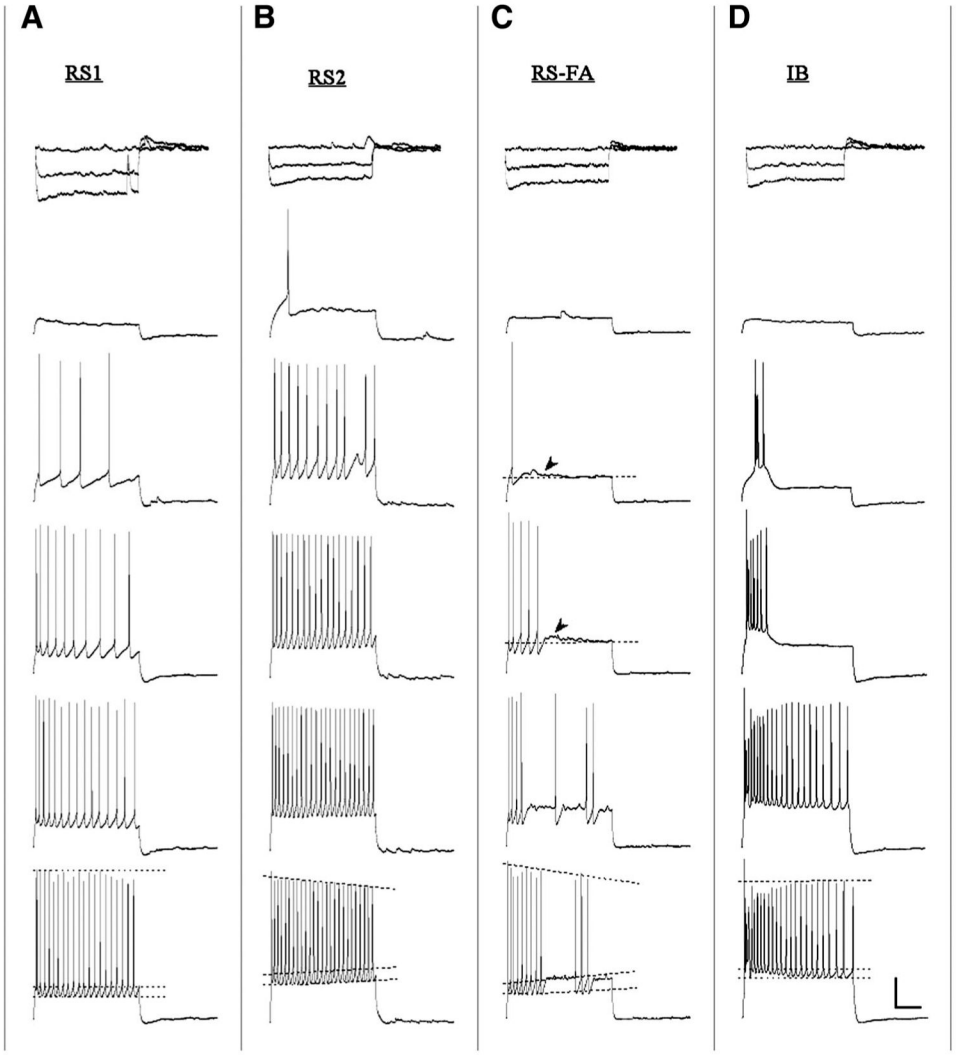

FIG. 2.

Distinctive repetitive AP firing patterns of representative RS1, RS2, FA, and intrinsically bursting (IB) cells. *A*: RS1 cells show little change in AP amplitude and threshold over trains evoked by 2-s current stimuli (30, 80, 130, 180, and 280 pA top to bottom). *B*: RS2 cells demonstrate increased AP threshold and decreased AP amplitude over time across each step. *C*: FA cells demonstrate marked firing rate adaptation and increased AP threshold and decreased AP amplitude during a train; arrowheads indicate the small depolarizing plateau observed after either a single spike or a spike train. *D*: IB cells demonstrate a pronounced burst of APs followed by a train of APs similar to those seen in RS1 cells. *Top traces* for each cell type represent the voltage response to hyperpolarizing steps (−120, −90, and 0 pA) Scale bar: 20 mV/500 ms.

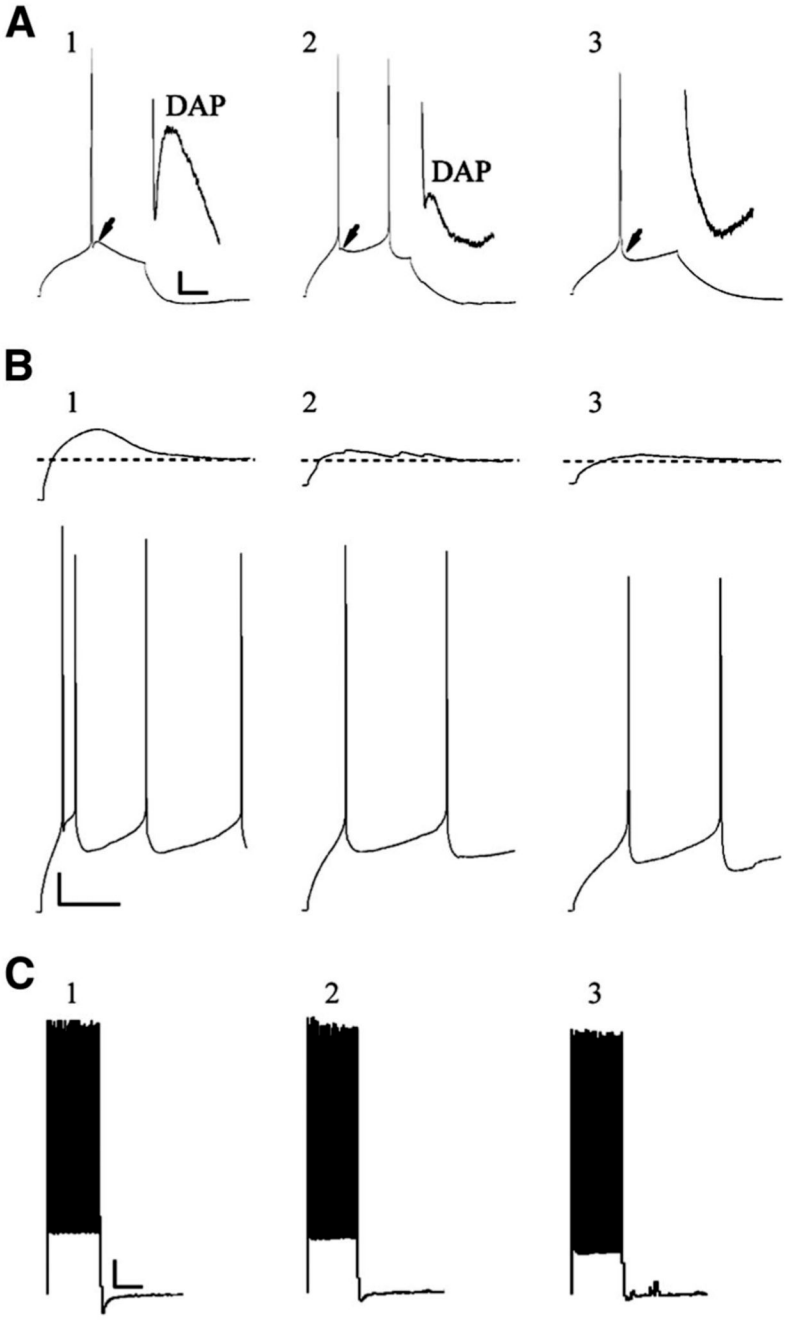

FIG. 3.

Three subclasses of RS1 cells. *A*: APs evoked by a 200-ms current step in low-threshold spiking (LTS, *A1*), intermediate RS1 (IM, *A2*), and non-LTS (*A3*) cells: scale bar; 10 mV/50 ms. LTS cells (↓ and *A1*, *inset*) and IM cells (↓ and *A2*, *inset*) exhibit a prominent depolarizing afterpotential (DAP). Non-LTS cells do not exhibit a DAP (↓and *A3*, *inset*). *B*: LTS cells show a large low-threshold depolarizing potential (*B1*, *top*) on which rides an AP doublet/triplet (*B1*, *bottom*: scale bar; 10 mV/200 ms) in response to 2-s, 30- and 80-pA current steps, respectively. IM cells (*B2*) and non-LTS cells (*B3*) lack a prominent low-threshold depolarizing potential and initial doublet. *C*: LTS (*C1*), IM (*C2*), and non-LTS (*C3*) cells all exhibit RS1

cells characteristics in response to a 2-s 180-pA depolarizing current step: scale bar: 10 mV/ 1,000 ms.

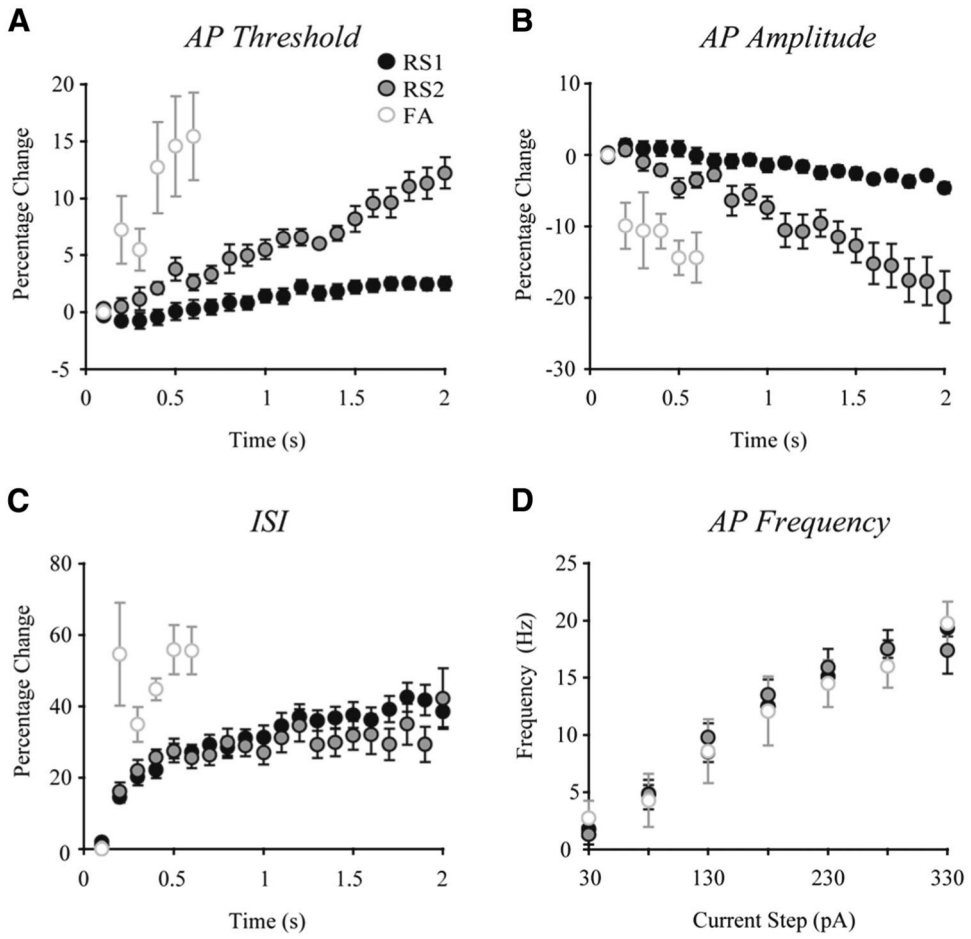

FIG. 4.

Characteristics of repetitive firing by RS1, RS2, and FA cells. *A*: AP thresholds increased to a significantly greater extent over the course of a train in RS2 and FA cells than in RS1 cells. *B*: AP amplitudes decreased to a significantly greater extent in RS2 and FA cells than in RS1 cells over the course of a train. *C*: interspike interval (ISI) durations were significantly longer in FA than in RS1 and RS2 cells. *D*: there were no significant differences among the 3 cells types in mean AP firing frequency during a given train of spikes evoked by increasing depolarizing current steps.

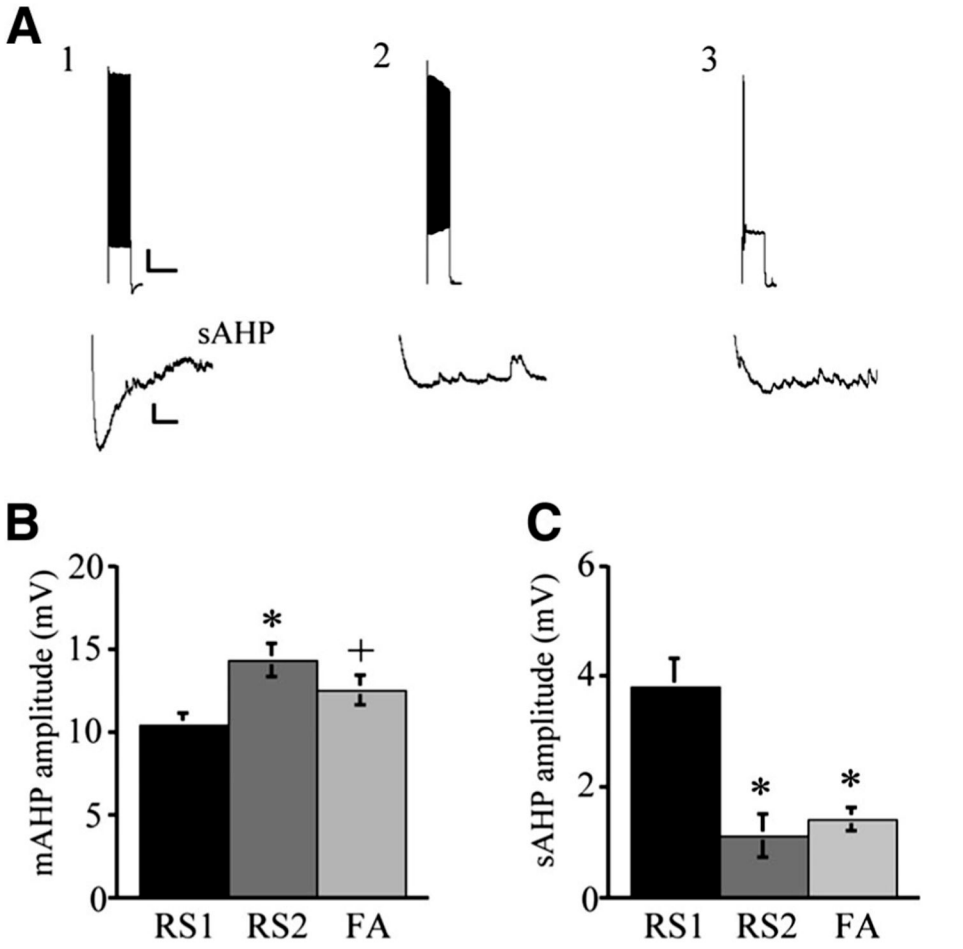

FIG. 5.

AHP characteristics of RS1, RS2, and FA type cells. *A*: slow afterhyperpolarization (AHP, *bottom*) followed trains of APs evoked by a 2-s current step of 330 pA. *A1*: prominent slow AHP was seen in RS1 but not RS2 (*A2*) or FA (*A3*) cells. Scale bars: 10 mV/2 s, *top*; 1 mV/10 ms, *bottom*. *B*: RS1 cells demonstrated a significantly lower medium AHP amplitude compared with RS2 (*$P < 0.004$) and showed a trend to be smaller than FA type cells (+$P < 0.08$). *C*: RS1 cells demonstrated significantly higher slow AHP amplitude compared with RS2 and FA cells (*$P < 0.001$).

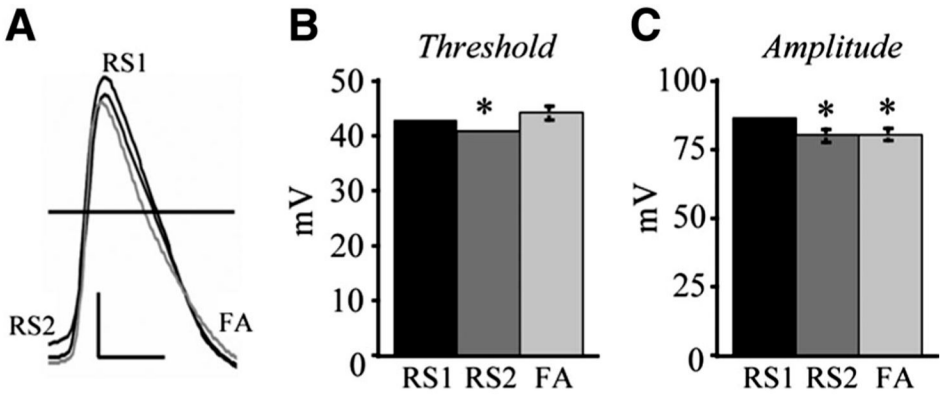

FIG. 6.

RS1 cells exhibit greater AP amplitude than RS2 and FA cells and lower AP threshold than RS2 cells. *A*: representative AP traces of individual RS1, RS2, and FA cells. Scale bar: 20 mV/1 ms. *B*: RS2 cells demonstrate a significantly lower AP threshold than the other 2 cell types (*RS2 vs. RS1, $P < 0.04$; RS2 vs. FA, $P < 0.05$). *C*: RS1 cells demonstrate significantly higher AP amplitude than RS2 (*$P < 0.03$) and FA cells (*$P < 0.04$).

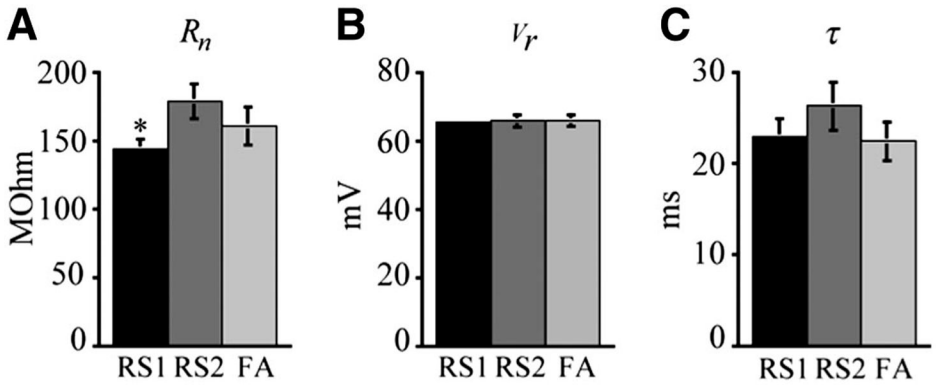

FIG. 7.

Passive membrane properties of the 3 RS cell types. *A*: bar graph demonstrating that input resistance was significantly lower in RS1 than in RS2 cells (**P* < 0.03) but not different between RS1 and FA or RS2 and FA cells. *B*: bar graph demonstrating that there was no difference in resting membrane potential among the 3 cell types. *C*: bar graph demonstrating that there was no difference in membrane time constant among the 3 cell types

TABLE 1

Electrophysiological characteristics of layer 5 cell types

	RS1	RS2	FA	IB
AP threshold across a train	No change	Increase	Increase	No change
AP amplitude across a train	No change	Decrease	Decrease	No change
ISI change across a train	Increase	Increase	Increase	Increase
Adaptation across 2-s depolarization	Slow	Slow	Fast	Slow
DAP	Present (72)	Absent	Absent	Present
Initial doublet	Present (59)	Absent	Absent	N/A
Sag	Present	Present	Present	Present
sAHP	Large	Small	Small	Large
mAHP	Small	Large	Large	Small

Values in parentheses are percentages; AP, action potential; ISI, interspike interval; DAP, depolarizing after potential; sAHP and mAHP, slow and medium after hyperpolarization.

TABLE 2

Morphologic characteristics of layer 5 cell types

	RS1	RS2	FA	IB
Basilar dendrites				
No. of 1° branches	6.2 ± 3.1	6.0 ± 2.7	7.0 ± 0.0	5.0
No. of branches	25.0 ± 8.5	19.3 ± 2.1	22.0 ± 8.2	11.0
No. of ends	33.0 ± 11.9	27.8 ± 2.5	30.0 ± 6.1	18.0
Mean length	687 ± 221	621 ± 234	440 ± 34	489
Total length, μm	3,851 ± 1,282	3,358 ± 574	3,083 ± 238	2,446
Apical Dendrite				
No. of branches	18.0 ± 4.6	20.0 ± 8.8	21.3 ± 4.2	11.0
No. of ends	19.8 ± 5.7	22.3 ± 8.6	23.0 ± 3.5	12.0
Total length, μm	3,688 ± 916	4,434 ± 1,280	3,556 ± 755	2,110
Soma				
Perimeter, μm	62.6 ± 12.8	60.7 ± 13.4	85.6 ± 6.5	74.2
Area, μm^2	252 ± 83	247 ± 100	446 ± 92	304

Values are means ± SD. *n* = 6 RS1, 4 RS2, 4 FA, 1 IB. RS1 and RS2, regular-spiking, slowly adapting type-1 and 2 FA, regular-spiking fast adapting; IB, intrinsically bursting.